Plant Physiology and Biochemistry 144 (2019) 413–426

Contents lists available at ScienceDirect

Plant Physiology and Biochemistry

journal homepage: www.elsevier.com/locate/plaphy

Research article

Untargeted metabolomic profiling reveals that different responses to self and cross pollination in each flower morph of the heteromorphic plant *Plumbago auriculata*

Di Hu[1], Wenji Li[1], Suping Gao[*], Ting Lei, Ju Hu, Ping Shen, Yurong Li, Jiani Li

Landscape Research Institute, Sichuan Agricultural University, Huimin Road 211, Wenjiang District, Chengdu, 611130, China

ARTICLE INFO

Keywords:
Fluorescence microscopy
HetSI
Non-targeted metabolomic analysis
Plumbago auriculata lam
Pollen-stigma interaction
Scanning electron microscopy
UPLC-MS/MS

ABSTRACT

Heteromorphic self-incompatibility (HetSI), which is regulated by sporophytes, occurs in some species as a strategy to promote cross-pollination. This research aimed to reveal metabolic changes occurring in HetSI. We used fluorescence microscopy as a tool to compare growth behavior in self-incompatible (SI) and self-compatible (SC) pollination in both pin and thrum flowers of *Plumbago auriculata* and to identify the ideal timepoint for sample collection for subsequent experiments. We also employed scanning electron microscopy (SEM) to evaluate intermorph structural differences in the pollen grains and stigmas in relation to HetSI. Importantly, UPLC-MS/MS was applied in this study to identify metabolites, compare metabolic differences between pin and thrum styles and monitor metabolic changes in SC and SI pollinations in the two types of flowers. The metabolites mainly included amino acids/peptides, flavonoids, glycosides/sugars, phenols, other organic acids, fatty acids (derivatives)/lipids, amines, aldehydes, alkaloids, alcohols and other compounds. Surprisingly, energy-related nutrients such as amino acids/peptides and tricarboxylic acid cycle-related metabolites were found at higher levels in SI pollinations than in SC pollinations. This result indicates that physiological changes in pollen-stigma interactions differ in pin and thrum styles and SC and SI pollinations and that energy deficiency is not one of the reasons for HetSI.

1. Introduction

Heterostyly is a genetic polymorphism comprising distylous or tristylous mating types that differ in reciprocally arranged female and male reproductive organs and promote disassortative pollination via segregated pollen deposition onto pollinators (Darwin, 1862; Kohn and Barrett, 1992; Lloyd and Webb, 1992). Distylous species have two floral morphs: pin (stigma above anthers) and thrum (stigma below anthers) (Fig. 1). According to Barrett (1992), heterostyly is one of the strategies used to promote cross-pollination for perfect flowers. Heterostyly accompanied by self-incompatibility (SI) acts as a safeguard against self-fertilization and inbreeding depression to increase the outcrossing rate (Darwin, 1862; Barrett and Cruzan, 1994), which is called heteromorphic self-incompatibility (HetSI).

Pistils are composed of the stigma, style and ovary. Compatible fertilization includes successful pollen-stigma recognition, pollen grain germination, pollen tube migration, and arrival at the ovary; however, self-incompatibility occurs when fertilization fails with disruption of any of these events. The self-incompatibility mechanism comprises homomorphic (HomSI) and heteromorphic (HetSI) self-incompatibility. HomSI has been widely studied in terms of morphology, transcriptomes, proteomes, and metabolomes (Faehnrich et al., 2015; Mondragon et al., 2017; Samuel et al., 2008; Zhao et al., 2016). Although, the research on heteromorphic self-incompatibility systems has a long history, especially in the genus *Primula*, and although much work has been done on the morphology, genetics, genomics, proteomics and transcriptomics of HetSI systems (Burrows and McCubbin, 2017; Costa et al., 2019; Lu et al., 2018; Stevens and Murray, 1981; Takeshima et al., 2019), there is no evidence to establish the metabolic mechanism of HetSI.

Genetic information may be reflect in the metabolome, and a single metabolite might influence gene expression, protein stability and metabolic fluxes (Fernie, 2007; Fiehn, 2002; Kim et al., 2011). Ultra-performance liquid chromatography-tandem mass spectrometry (UPLC-

* Corresponding author.
E-mail addresses: gailhu@163.com (D. Hu), liwenjilwj@126.com (W. Li), gao_suping@sicau.edu.cn (S. Gao), ting_lei85@sicau.edu.cn (T. Lei), huju918@yahoo.com (J. Hu), 18428385614@163.com (P. Shen), yellor326815@163.com (Y. Li), zaq135@126.com (J. Li).
[1] These authors contributed equally to this work.

https://doi.org/10.1016/j.plaphy.2019.10.010
Received 22 July 2019; Received in revised form 8 October 2019; Accepted 8 October 2019
Available online 12 October 2019

Abbreviations

SI	self-incompatibility
SC	self-compatibility
HetSI	heteromorphic self-incompatibility
HomSI	homomorphic self-incompatibility
TS	the styles of thrum flowers
PS	the styles of pin flowers
P × P	pin-morph stigmas pollinated with pin pollens
P × T	pin-morph stigmas pollinated with thrum pollens
T × T	thrum-morph stigmas pollinated with thrum pollens
T × P	thrum-morph stigmas pollinated with pin pollens
The P group	PS, P × P, P × T
The T group	TS, T × T, T × P
The SC group	P × T and T × P
The SI group	T × T, P × P
UPLC-MS/MS	Ultra-performance liquid chromatography-tandem mass spectrometry
SEM	scanning electron microscopy
FM	fluorescence microscopy
PCA	principal component analysis
OPLS-DA	orthogonal partial least squares-discriminate analysis
PLS-DA	partial least squares-discriminant analysis
TCA	tricarboxylic acid cycle
QC	quality control
ANOVA	analysis of variance

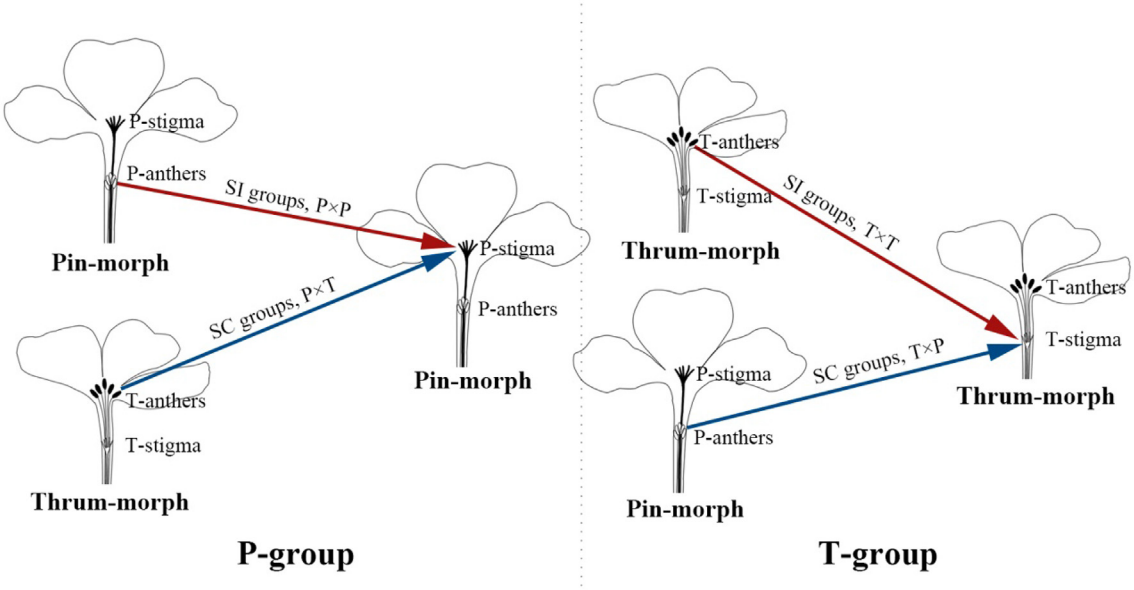

Fig. 1. Pin-morph flower (P) and thrum-morph flower (T). The P group (PS: the styles of pin flowers; P × P: pin-morph stigmas pollinated with pin pollens; P × T: pin-morph stigmas pollinated with thrum pollens). The T group (TS: the styles of thrum flowers; T × T: thrum-morph stigmas pollinated with thrum pollens; T × P: thrum-morph stigmas pollinated with pin pollens). The red arrows indicate self-incompatible (SI) pollinations and the blue arrows self-compatible (SC) pollinations. (For interpretation of the references to colour in this figure legend, the reader is referred to the Web version of this article.)

MS/MS) is a powerful technique for identifying metabolites in plants (Zhang et al., 2017), and untargeted scanning is invaluable for identifying a large set of metabolites and understanding metabolic and physiological processes in plant physiology (Jiao et al., 2018).

Plumbaginaceae, a cosmopolitan family contains 25–30 gernera and 650–1000 species (Hernández-Ledesma et al., 2015; Mucina and Hammer, 2019). Heterostyly is known to occur in several genera of the family, including *Acantholimon*, *Armeria*, *Goniolimon*, *Limoniastrum*, *Limonium*, *Ceratostigma*, *Dyerophytum* and *Plumbago* (Baker, 1953a,b; Dulberger, 1975). Due to the variation of distylous species, members of Plumbaginaceae provide an ideal system for investigating heterostyly, and *Plumbago auriculata* Lam. (Plumbaginaceae), a typical HetSI plant, is included in this family. This is the first study to assess morphological differences, identify metabolites and monitor metabolic changes in *P. auriculata* during different pollinations in an attempt to characterize biochemical changes that occur with different pollination treatments and to provide supplementary data for the HetSI mechanism.

2. Material and methods

2.1. Materials and reagents

Floral styles were collected from samples of *Plumbago auriculata* pollinated in different manners (PS, TS, P × P, P × T, T × T, T × P). More than 600 plants were grown in a greenhouse at Sichan Agricultural University for generations. Anthers of the randomly selected flowers were emasculated the day before dehiscence, and flowers were isolated with bag exclusions to exclude pollinators and prevent predation before pollination. Styles for morphological study were manually pollinated at 8:00 a.m. (P × P, P × T, T × T, and T × P) and collected after 1, 2, 4, and 8 h (fifty pollinated styles were collected at each time point in different pollination treatments). Pin and thrum styles for metabolome analysis were collected without any type of pollination treatment (a total of 400 styles were prepared for each type) at 10:00 a.m. For metabolome analysis, styles were manually pollinated at 8:00 a.m. and collected after 2 h (10:00 a.m.). A total of 400 (approximately 400 mg) pollinated styles were prepared for each pollination treatments (P × P, P × T, T × T, and T × P).

2.2. Staining and microscopy

2.2.1. Fluorescence microscopy

To examine differences in pollen tube growth in SI and SC groups, the growth behaviors of pollen tubes of *P. auriculata* were observed by fluorescence microscopy (FM). Floral styles at 1, 2, 4, and 8 h after pollination were collected and fixed in ethanol:acetic acid (2:1, v:v) for

12 h. The fixed stigmas were cleared with 8 mol/L NaOH for 6 h, rinsed thoroughly in distilled water, washed three times with K_3PO_4 (0.1 mol/L), soaked for 20 min and stained with 0.05% achromatic aniline blue. Pollen grain and stigma interactions were detected by fluorescence microscopy (BX53 + DP80, Olympus, Japan). Each experiment was replicated 30 times.

2.2.2. Scanning electron microscopy

The distinguishing characteristics between pollen grain and stigmas might be due to secondary characteristics in the SI process. Scanning electron microscopy (SEM) was used to observe SC and SI pollen-stigma interactions of *P. auriculata*. Fresh samples of styles from P × P, P × T, T × T, T × P pollinations were directly adhered onto stages using conducting resin and placed in a special low-pressure chamber of a FEI (America) Quanta 250 microscope. For observation, the pressure was set to 150 Pa, and the tension was set to 500 kV. Micrographs were interpreted automatically using the hardware and software supplied with the microscope. Each experiment was replicated five times.

2.3. Sample preparation and extraction

Two-hour-pollinated styles were randomly collected from different pollination treatments (50 styles for each sample) and immediately frozen in liquid nitrogen and stored at −80 °C for metabolite extraction. Eight biological replicates were prepared for this research. All samples were ground into homogeneous powder (50 mg for each sample), which was then extracted with 1 ml of methanol:acetonitrile:water (2:2:1, v:v:v) to form a turbid suspension that was ultrasonically treated twice for 30 min at ultralow temperature. The sample was incubated for 1 h at −20 °C for protein precipitation. After centrifugation at 13,000 rpm for 15 min at 4 °C, the supernatant was completely removed using a vacuum concentrator. The sample was redissolved in 100 µl of acetonitrile:water (1:1, v:v) and centrifuged at 14,000 g for 15 min at 4 °C. The supernatant was injected directly into the UPLC system. The volume injected for each run was 10 µl. A quality control (QC) sample was prepared by mixing aliquots from each of the samples.

2.4. UPLC-MS/MS

To explore the relationship between metabolic changes and the mechanism of HetSI, UPLC-MS/MS was performed on style extracts of different pollination treatments.

UPLC analysis was performed using an Agilent (America) 1290 Infinity LC UPLC system with the Waters (America), ACQUITY UPLC BEH Amide 1.7 µm, 2.1 mm × 100 mm column. The mobile phases consisted of eluents A (water + 25 mM ammonium acetate + 25 mM ammonia water) and B (acetonitrile), with a flow rate of 0.3 ml/min and a linear gradient program as follows: 95% B from 0 to 0.5 min, 95%–65% B from 0.5 to 7 min, 65%–40% B from 7 to 9 min, B maintained at 40% from 9 to 10 min, 40%–95% B from 10 to 11.1 min, and B remaining at 95% from 11.1 to 16 min. The temperature of the UPLC column and autosampler were set at 25 °C and 4 °C, respectively.

The MS experiments were performed using a Triple-TOF 5600+

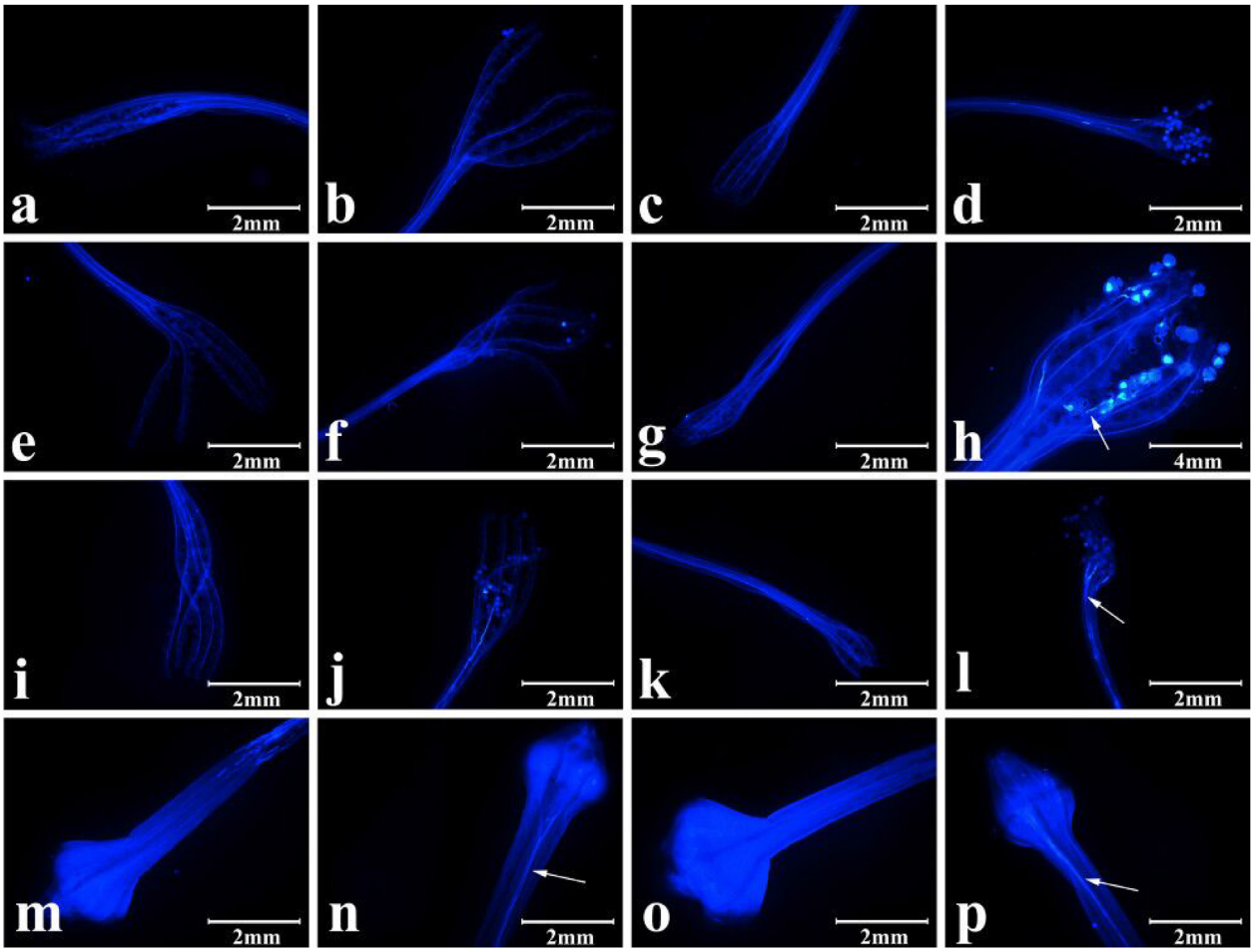

Fig. 2. The development of pollen tubes after 1, 2, 4, and 8 h in SI and SC pollination. (a, e, i, m) P × P pollinations, 1 h, 2 h, 4 h, and 8 h from top to bottom; (b, f, j, n) P × T pollinations, 1 h, 2 h, 4 h, and 8 h from top to bottom; (c, g, k, o) T × T pollinations, 1 h, 2 h, 4 h, and 8 h from top to bottom; (d, h, l, p) T × P pollinations, 1 h, 2 h, 4 h, and 8 h from top to bottom. The direction of the white arrows indicates the position of the pollen tube.

mass spectrometer (AB SCIEX, America) connected to the UPLC system through an electrospray ionization (ESI) interface. The optimized instrumental parameters were as follows: ion source gas1 (Gas1), 60; ion source gas2 (Gas2), 60; curtain gas (CUR), 30; source temperature, 600 °C; ion spray voltage floating (ISVF), ± 5500 V (positive/negative mode); TOF MS scan m/z range, 60–1200 Da; product ion scan m/z range, 25–1200 Da; TOF MS scan accumulation time, 0.15 s/spectrum; and product ion scan accumulation time, 0.03 s/spectrum. Secondary mass spectrometry data were acquired using information dependent acquisition (IDA) in high-sensitivity mode with declustering potential (DP) of ± 60 V (positive/negative mode), collision energy of 30 eV; IDA excluded isotopes within 4 Da, and 6 candidate ions were monitored per cycle. The QCs were injected at regular intervals (every 8 samples) throughout the analytical run to provide a set of data.

2.5. Data analysis

For the screening analysis, raw data were transferred to. mzXML files using ProteoWizard. The XCMS program was applied for assessing peak alignments, retention time corrections, and peak area extraction. A tolerance of mass accuracy (< 25 ppm) and second-order spectrum matching were applied to identify the chemical structures of metabolites. The resulting data were analyzed by PCA, OPLS-DA, PLS-DA and the *t*-test. Information for chemical compounds were obtained from mass spectra, retention times, a self-built database and METLIN. Metabolites were compared by peak areas. Heatmaps were generated in R-language. Eight biological replicates were treated as an average per sample for subsequent metabolite analysis.

3. Results

3.1. Growth behaviors of pollen tubes in compatible and incompatible groups

The pollen grain germinated at approximately 2 h (Fig. 2h) only on SC stigmas; however, a longer period of time was required for germination of the SC pollen in the P group, and no pollen germination was observed at this timepoint for SI pollen (Fig. 2e and g). Pollen tubes in both pin and thrum flowers were elongated at approximately 4 h (Fig. 2j and l) and reached the ovary within 8 h (Fig. 2n and p). Conversely, no SI pollen stably adhered onto stigmas. According to the results, 2 h appears to be the ideal timepoint to detect differences between HetSI mechanisms.

3.2. Pollen-stigma interactions in compatible and incompatible groups

To ensure sufficient time for the pollen grain and stigmas to interact, pollen germination was examined approximately 2 h after artificial pollination. The “foot” structures (pollen-stigma cross-linking) penetrating the stigmas through papillae can be clearly observed in T × P pollinations (Fig. 3c). Interestingly, P × T pollinations showed a distinct morphology; the stigmatic papillae around the germinated pollen became less globular (Fig. 3a), and no “foot” structure was observed. In contrast, no pollen tubes and no shriveled stigmatic papillae were discovered in SI pollinations (Fig. 3b and d).

3.3. Metabolite identification by UPLC-MS/MS

Successful pollen adherence and hydration appear to be key points for successful fertilization in *P. auriculata*, and samples for metabolite extraction were collected at 2 h after artificial pollination to assess differences between self-incompatibility and self-compatibility.

UPLC-MS/MS of the *P. auriculata* style metabolome revealed 142

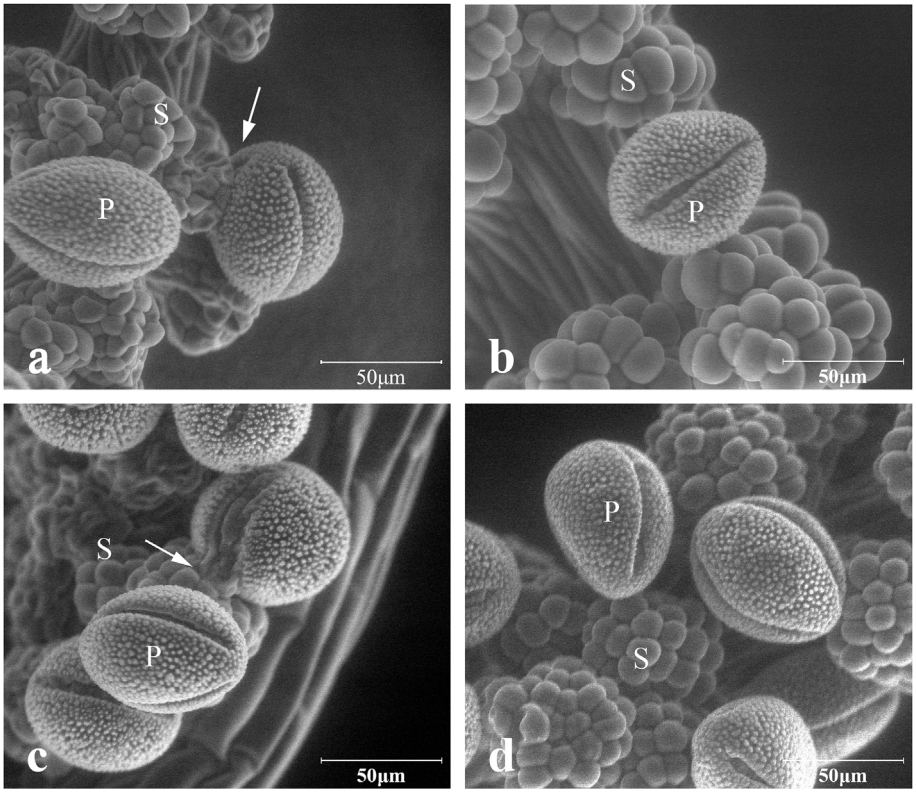

Fig. 3. Pollen-stigma interactions after different pollinations for 2 h. (a) P × T; (b) P × P; (c) T × P; (d) T × T. The direction of the white arrows indicates the position of the stigma-pollen cross-linking. P: pollen; S: stigma.

named metabolites identified or tentatively characterized in both positive and negative modes (Table S1). The total ion chromatograms (TIC) are shown in Fig. 4. More specifically, PS (styles of the pin flowers), TS (styles of the thrum flowers), P × P, P × T, T × T, and T × P samples mainly yielded amino acids/peptides, flavonoids, glycosides/sugars, phenols, amines, other organic acids, fatty acids (derivatives)/lipids, aldehydes, alkaloids, alcohols and other compounds. A quality control (QC) sample was also generated to provide a set of data from which repeatability was assessed.

3.4. Different pollination treatments showed distinct metabolite levels

Principal component analysis (PCA) 2D plots of results from the 6 groups illustrated clear separation of the pollination samples into clusters according to their common spectral characteristics (Fig. 5). This result means that the 6 groups can be easily differentiated.

Statistical analysis (OPLS-DA, PLS-DA and *t*-test) was performed to calculate variations. In the comparison of the PS and TS, there were significant changes in the levels of 82 (VIP $>$ 1, *P* value $<$ 0.05) compounds. In the comparison of the T × T and T × P, there were significant changes in the levels of 67 (VIP $>$ 1, *P* value $<$ 0.05) compounds, and in the comparison of the P × T and P × P, there were significant changes in the contents of 67 metabolites (Table 1).

A heatmap was generated (Fig. 6), which revealed marked variation in metabolite abundance for the different pollination treatments. Correspondingly, an obvious separation could be observed between styles without pollinations (PS, TS) and pollinated styles (P × P, P × T, T × P, T × T). In Fig. 6a, PS and TS were grouped into 2 classes. In Fig. 6b the 32 samples were mainly grouped into 4 subclasses consisted of samples from styles in different pollination treatments (P × P, P × T, T × P, T × T).

3.4.1. Amino acids/peptides

Twenty-one types of amino acids/peptides were detected, and their

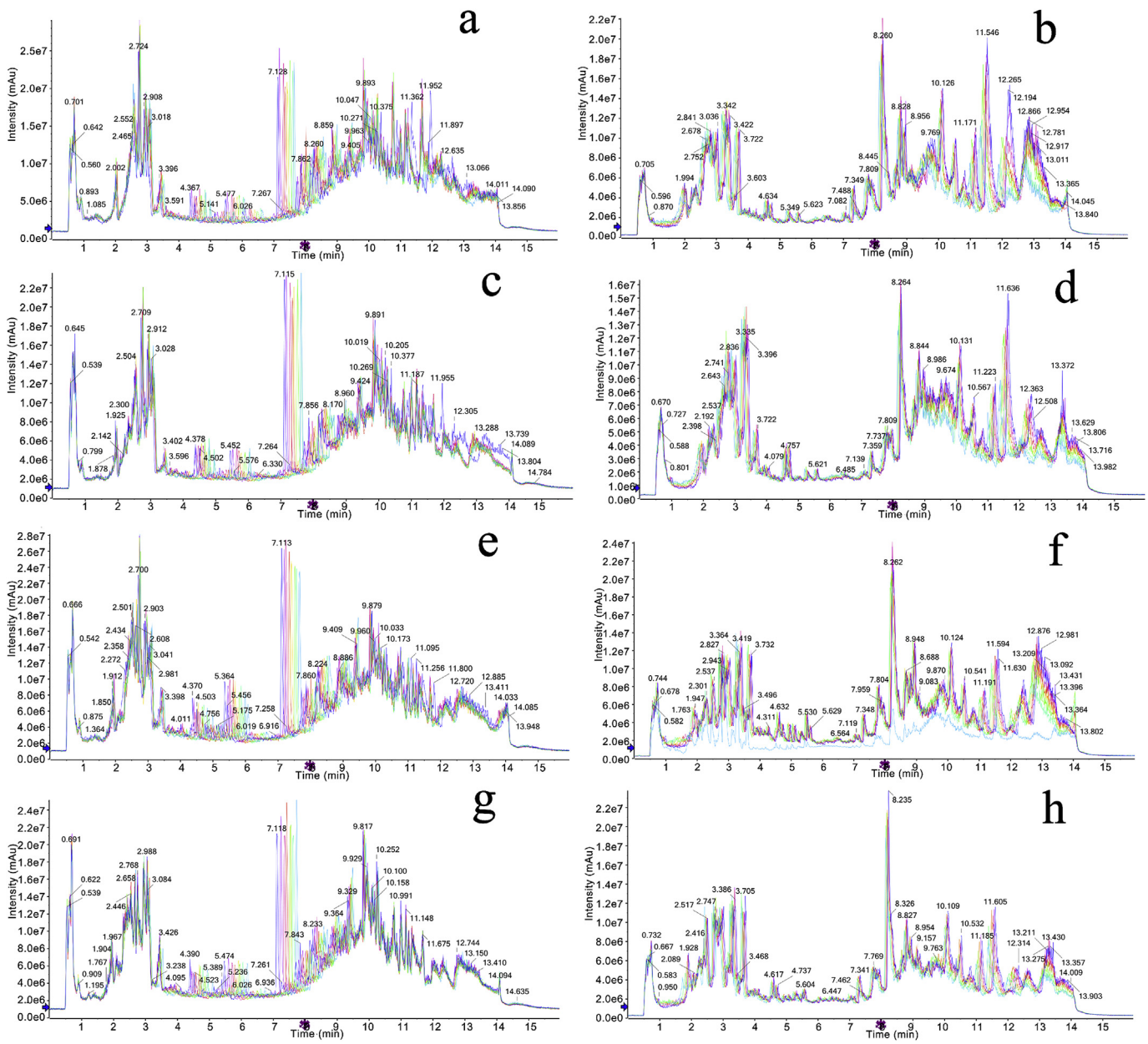

Fig. 4. Total ion chromatograms from different pollinations (positive and negative modes). (a) PS positive mode; (b) PS negative mode; (c) TS positive mode; (d) TS negative mode; (e) P × P positive mode; (f) P × P negative mode; (g) P × T positive mode; (h) P × T negative mode; (i) T × T positive mode; (j) T × T negative mode; (k) T × P positive mode; (l) T × P negative mode, (m) QC positive mode; (n) QC negative mode.

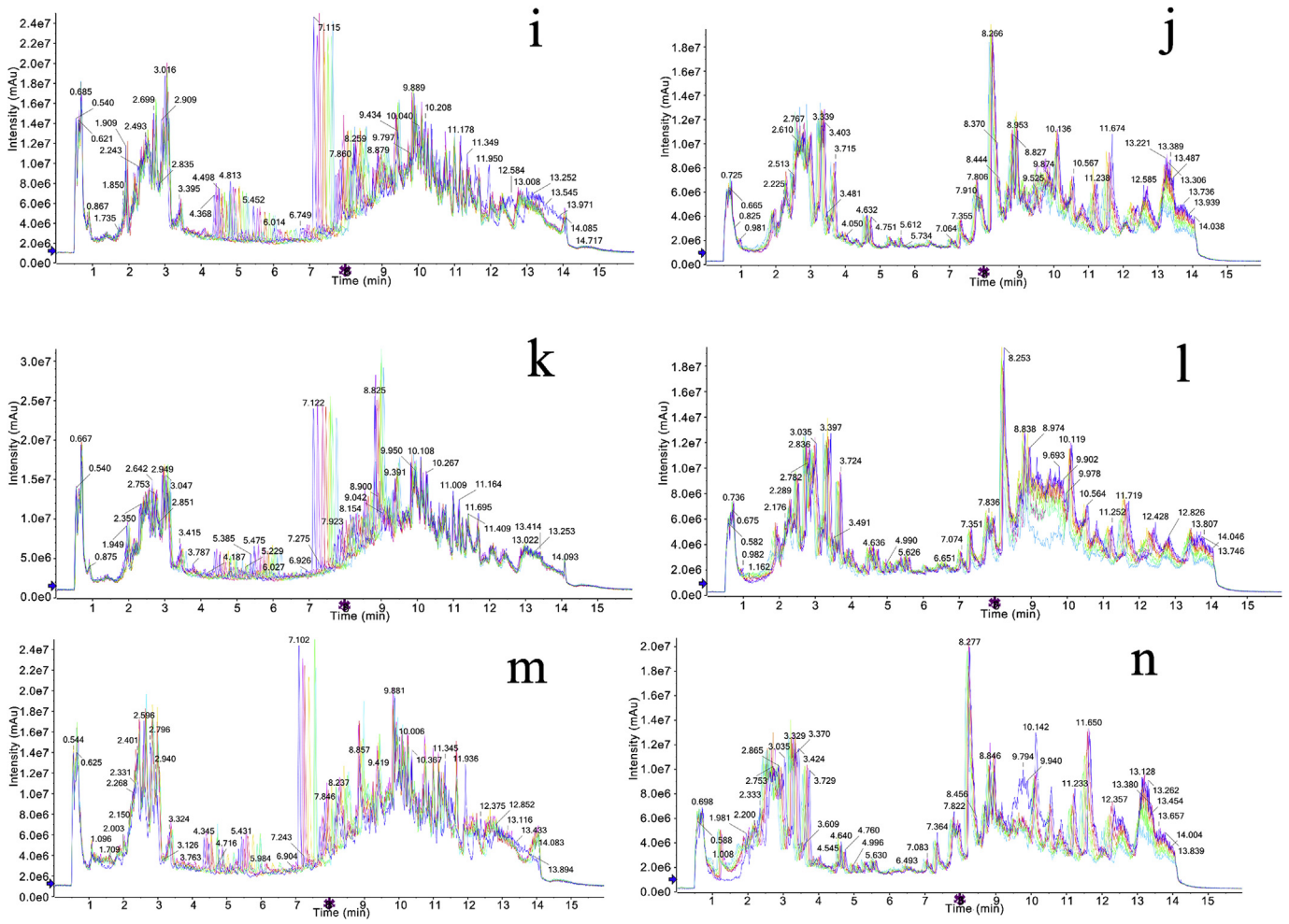

Fig. 4. (*continued*)

levels were compared between the PS and TS groups (Table S1). The total content of amino acids/peptides was higher in TS (Fig. 7a). Fourteen types of amino acids/peptides showed significant changes (VIP > 1, *P* value < 0.05) in relative content (Table 1). Glutamine, glutathione, glutamic acid, isoleucine, N-acetyl-L-phenylalanine, prolyl-tryptophan, aspartic acid, pipecolic acid, lysine and N-acetyl-L-aspartic acid showed distinct increases in TS, whereas only glutathione disulfide, tyrosine, isoleucyl-proline and leucyl-phenylalanine were higher in PS.

Compared with the levels in T × P, 6 types of amino acids/peptides showed distinct increases in T × T: glutathione, phenylalanine, tyrosine, leucyl-phenylalanine, pipecolic acid and N-acetyl-L-aspartic acid (Table S1). Unsurprisingly, a similar trend in total amino acids/peptides contents was observed for P × T and P × P (Fig. 7a). Levels of glutathione, arginine, histidine, isoleucine, N-acetyl-L-aspartic acid, N-acetyl-L-phenylalanine, tryptophan, isoleucyl-proline, leucyl-phenylalanine, leucyl-leucine, pipecolic acid and lysine were changed significantly.

3.4.2. Flavonoids

Compare with PS, the total content of flavonoids showed distinct increases in TS (Fig. 7b). Myricetin, myricitrin, catechin and procyanidin B2 changed significantly and were more abundant in TS. However, 3-O-methylquercetin, kaempferol, kaempferol-3-O-rutinoside, rutin, quercitrin, quercetin, isorhamnetin and isoquercitin decreased sharply (Table S1).

In T × T and T × P, flavonoids levels changed significantly. Compared with SC pollinations, myricetin increased in SI pollinations, whereas taxifolin, 3-o-methylquercetin, kaempferol, kaempferol-3-o-rutinoside, isorhamnetin, procyanidin b2 and rutin decreased sharply. In the pin-female parent group, 3-o-methylquercetin and isorhamnetin increased in the SI group, but kaempferol, kaempferol-3-o-rutinoside, myricetin, quercetin, procyanidin b2, myricitrin and rutin remained low (Table S1).

3.4.3. Glycosides/sugars

The levels of glycosides/sugars remained higher in TS (Fig. 7c), and 6 types of glycosides/sugars showed significant changes (VIP > 1, *P* value < 0.05) when the PS and TS groups were compared (Table 1). Adenosine monophosphate (AMP), nicotinamide adenine dinucleotide phosphate (NADP) and glucoronate were increased in TS, whereas guanosine, inosine and S-methyl-5′-thioadenosine decreased (Table S1).

The content of glycosides/sugars in the SC and SI groups included AMP, adenosine, glucuronate, mannose, trehalose, guanosine, inosine, alpha-hederin, xanthosine, maltose, sucrose, alpha-D-galactose 1-phosphate, nicotinamide adenine dinucleotide phosphate (NADP), uridine 5′-diphospho-N-acetylgalactosamine and S-methyl-5′-thioadenosine (Table S1). The total content was much higher in the SC group than in the SI group (Fig. 7c).

3.4.4. Other organic acids

A total of 34 other organic acids were detected (Table S1). Unsurprisingly, compared with PS, other organic acids remained at higher levels in TS, and 18 showed significant changes (VIP > 1, *P* value < 0.05) (Table 1). TCA intermediates such as citrate and malic acid were all abundant in TS (Fig. 7i) (Table S1).

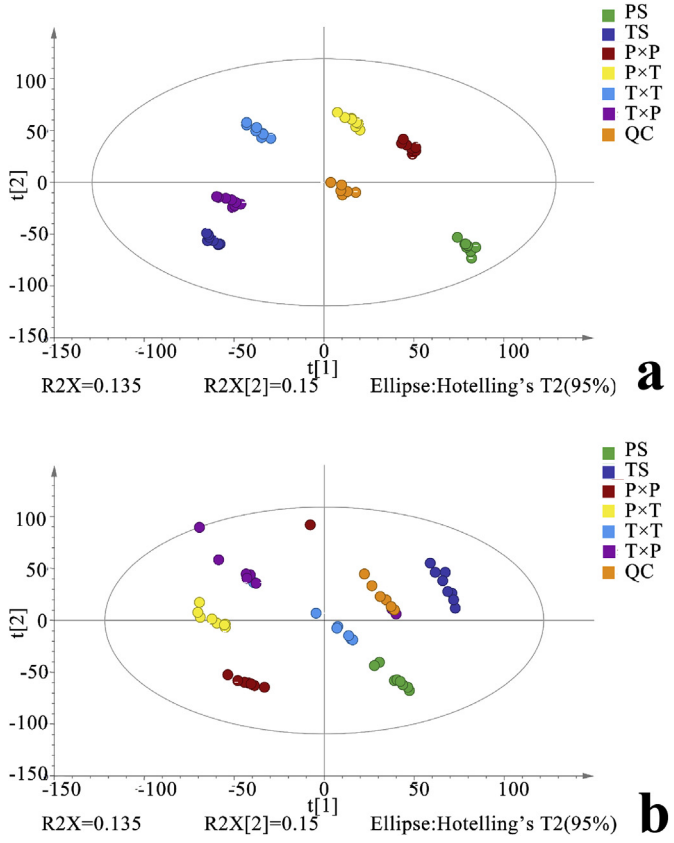

Fig. 5. PCA of different pollinations in positive mode (a) and negative mode (b) (●). group on PS samples (●); group on TS samples (●); group on P × P samples (●); group on P × T samples (●); group on T × T samples (●); group on T × P samples (●); group on QC samples.

Intermediates of the TCA cycle (citrate, isocitrate, malic acid and aconitate) included other organic acids. In T × T and T × P, intermediates of the TCA cycle were present at much higher levels in the SI group than in the SC group. Unsurprisingly, the same trend was found in P × P and P × T (Fig. 7i).

3.4.5. Fatty acids (derivatives)/Lipids

Thirty-one named fatty acids (derivatives)/lipids were detected, including 17 that showed significant changes (Table 1). Cutin, suberin and wax biosynthesis of 16-hydroxypalmitic acid remained higher in TS. However, fatty acid biosynthesis of linoleic acid decreased in TS compared with PS (Table S1).

After SI pollination, the total content of fatty acids (derivatives) increased in the T group, and the corresponding content in the P group showed the opposite trend (Fig. 7e).

3.4.6. Alcohols

Four types of alcohols were detected (Table S1). Among them, phytosphingosine, uvaol and ascorbic acid showed significant changes (Table 1). The content of phytosphingosine increased in TS, and ascorbic acid metabolism showed the same trend in TS (Table S1).

The alcohol content showed an opposite tendency in the T and P groups, with higher levels in SC pollinations than in SI pollinations in the T group but higher levels in SI pollinations in the P group (Fig. 7f).

3.4.7. Amines

Amines were more abundant in TS than PS (Fig. 7h). Four types of amines changed significantly (Table 1). Betaine, one of the metabolites found in glycine, serine and threonine metabolism, showed distinct increases in TS, and glycerophosphocholine showed the same trend. Spermidine and phenylethylamine changed in an opposite manner (Table S1).

The total content of amines in SI pollinations was reduced compared to that in SC pollinations in the P groups and remained steady in the T groups (Fig. 7h). 3-Methoxytyramine, spermidine, tryptamine and tyramine were significantly altered in T × T and T × P. Four types of amines showed obvious changes in P × T and P × P (Table 1).

3.4.8. Other metabolites

Other metabolites included phenols, aldehydes, alkaloids and heterocyclic compounds. Phenols were richer in TS than in PS (Fig. 7g). Indole (heterocyclic compound), vanillin (aldehyde) and 3-formylindole (heterocyclic compound) remained higher in TS, whereas caffeine (alkaloid), 3-methyluric acid (alkaloid) and theobromine (alkaloid) showed the opposite trend (Table S1).

Some aldehydes such as phenylacetaldehyde decreased significantly in the T group after SI pollination, although vanillin increased. Compared with SC pollinations, an increase in uric acid (alkaloid) was observed in SI pollinations, whereas a higher level of 3-formylindole (heterocyclic compound) was found in SI pollinations. In addition, biliverdin (heterocyclic compound) remained richer in SI pollinations. The total content of phenols was much higher in SI pollinations than in SC pollinations (Fig. 7g); however, resveratrol and matairesinol significantly changed and remained more abundant in SI pollinations. In the P group, vanillin content decreased after SI pollination. Alkaloid (theobromine and 3-methyluric acid) was more abundant in SI pollinations. The total content of phenols increased after SC pollination (Fig. 7g), and phloretin decreased after SI pollination; however, resveratrol showed the opposite pattern (Table S1).

4. Discussion

The morphological study showed the microstructure of pollen-stigma interactions. No liquid was present on the stigma surface, precluding adhesion; thus, a dry-type stigma is typical. Furrows were absent on both types of pollens, there were no obvious changes in the volume of SC pollens after rehydration on stigmas and callose was present before germination (the blue highlight in Fig. 2 h), which might indicate partially hydrated pollens (with water content greater than 30% at shedding) (Franchi et al., 2007; Pacini et al., 2006). According to Franchi, *Parietaria* also has dry stigmas and partially hydrated pollens (Franchi et al., 2007). In SI pollinations, fertilization failed on the stigma, and no pollen tubes were observed penetrating the stigmas through papillae (Fig. 2 e, g). However, 2 h after SC pollinations, a pollen-stigma cross-linking was observed, which facilitates hydration and germination of the SC pollen as access to the inner surface of the stigma (Swanson et al., 2004). Much work has been done on cross-linking adhesions, and the results showed that glycoproteins play a key role in pollen-stigma cross-linking (Luu et al., 1999). The results indicate that glycoproteins may participate in the pollen-stigma interaction.

In the metabolomic study, 142 named metabolites were identified in 2 morphs of styles and 4 different pollination treatments. According to PCA, PS, TS, T × T, T × P, P × T and P × P were separated from each other, indicating that metabolites from the T group and the P group were clearly distinguished (Fig. 5). *P. auriculata* showed distinct metabolic differences for self-incompatibility in pin and thrum flowers.

The mature style stores a large amount of nutrients for pollen tube growth. The levels of TCA intermediates, amino acids/peptides, phenols, glycosides/sugars, alcohols, amines and flavonoids remained high in TS (Fig. 7), which indicates that a large amount of energy was provided to fuel pollen tube growth. According to the fluorescence microscopic observation, SC pollens have a faster growth rate on TS than on PS. This phenomenon may be related to the high levels of nutrients in TS.

Pollen tube growth is a highly energy-consuming process involving

Table 1
Significant differences in concentrations of detected metabolites in styles of different pollinations.

Metabolite		PS/TS		P × P/P × T		T × T/T × P	
		VIP	*P*.value	VIP	*P*.value	VIP	*P*.value
Amino acids/Peptides	Glutathione	**1.56**	**2.62E-08**	**1.38**	**7.07E-04**	**1.43**	**0.02**
	Glutamine	**1.54**	**1.24E-07**	0.28	0.57	**1.54**	**1.64E-05**
	Glutathione disulfide	**1.33**	**8.40E-05**	0.31	0.51	1.25	0.29
	Glutamic acid	**1.45**	**8.72E-06**	0.57	0.87	1.24	0.21
	Phenylalanine	0.66	0.13	0.87	0.05	**1.82**	**1.23E-03**
	Tyrosine	**1.32**	**1.27E-04**	0.91	0.05	**1.70**	**0.04**
	Arginine	0.02	0.96	**1.63**	**1.30E-07**	0.40	0.41
	Histidine	0.59	0.18	**1.44**	**8.31E-05**	0.93	0.04
	Isoleucine	**1.46**	**5.68E-06**	**1.40**	**1.77E-04**	0.36	0.46
	N-Acetyl-L-phenylalanine	**1.02**	**0.01**	**1.53**	**5.56E-05**	0.31	0.89
	Prolyl-Tryptophan	**1.44**	**1.18E-05**	0.38	0.43	0.21	0.67
	Tryptophan	0.92	0.03	**1.33**	**5.48E-04**	0.84	0.07
	Aspartic acid	**1.52**	**1.83E-07**	0.23	0.62	1.18	0.15
	Dimethylglycine	0.42	0.34	0.08	0.86	0.20	0.68
	Isoleucyl-Proline	**1.03**	**0.01**	**1.69**	**4.18E-10**	**1.40**	**3.46E-04**
	Isoleucyl-Tryptophan	0.81	0.05	0.31	0.50	0.30	0.53
	Pipecolic acid	**1.64**	**6.21E-16**	**1.64**	**7.32E-08**	**1.72**	**2.86E-09**
	Leucyl-Leucine	0.19	0.67	**1.11**	**0.01**	**1.17**	**0.01**
	Leucyl-phenylalanine	**1.65**	**2.29E-18**	**1.74**	**2.47E-19**	**1.35**	**7.64E-04**
	Lysine	**1.30**	**2.79E-04**	**1.55**	**3.44E-06**	0.59	0.21
	N-Acetyl-L-aspartic acid	**1.17**	**2.30E-03**	**1.27**	**3.14E-03**	**1.92**	**0.01**
Flavonoids	3-O-methylquercetin	**1.55**	**1.07E-07**	**1.04**	**0.02**	**1.75**	**0.02**
	Kaempferol	**1.64**	**1.65E-13**	**1.56**	**2.93E-06**	**1.35**	**7.26E-04**
	Myricetin	**1.49**	**1.45E-06**	**1.23**	**2.08E-03**	**1.41**	**3.38E-04**
	Rutin	**1.54**	**1.35E-07**	**1.59**	**9.24E-07**	**1.58**	**6.44E-06**
	Quercitrin	**1.34**	**1.38E-04**	0.20	0.66	0.86	0.06
	Quercetin	**1.49**	**2.42E-06**	**1.74**	**2.02E-08**	1.02	0.07
	Hyperoside	0.89	0.03	0.06	0.92	0.89	0.30
	Kaempferol-3-O-rutinoside	**1.57**	**1.09E-08**	**1.17**	**4.61E-03**	**1.45**	**1.57E-04**
	Myricitrin	**1.61**	**1.12E-10**	**1.11**	**0.01**	0.56	0.30
	Procyanidin C1	0.80	0.05	0.31	0.49	0.47	0.58
	Procyanidin B2	**1.60**	**9.73E-10**	**1.08**	**0.01**	**1.66**	**0.03**
	Isorhamnetin	**1.64**	**3.44E-14**	**1.63**	**1.00E-07**	**1.60**	**2.88E-06**
	Isoquercitin	**1.28**	**4.25E-04**	0.72	0.12	0.10	0.84
	Naringenin	0.96	0.02	0.95	0.03	0.32	0.50
	Taxifolin	0.40	0.36	0.57	0.22	**1.46**	**1.81E-05**
	Catechin	**1.11**	**4.27E-03**	0.46	0.32	0.15	0.76
	Epicatechin	0.12	0.78	0.87	0.05	0.65	0.17
Glycosides/Sugars	Adenosine monophosphate (AMP)	**1.08**	**0.01**	0.10	0.80	1.02	0.27
	Adenosine	0.54	0.22	**1.67**	**5.02E-09**	**1.70**	**1.72E-08**
	Glucuronate	**1.59**	**1.22E-09**	0.38	0.47	**1.77**	**0.03**
	Mannose	0.18	0.71	0.93	0.04	**1.81**	**0.02**
	Trehalose	0.42	0.31	0.28	0.59	**1.59**	**0.03**
	Guanosine	**1.23**	**6.42E-04**	**1.68**	**2.07E-09**	**1.56**	**1.06E-05**
	Inosine	**1.38**	**3.80E-05**	**1.28**	**2.80E-03**	1.38	0.08
	alpha-Hederin	0.84	0.05	0.65	0.17	0.36	0.62
	Xanthosine	0.50	0.24	0.22	0.66	0.93	0.33
	Maltose	0.38	0.39	0.48	0.30	0.60	0.21
	Sucrose	0.10	0.82	0.69	0.13	0.53	0.27
	alpha-D-Galactose 1-phosphate	0.36	0.37	0.30	0.53	**1.64**	**0.03**
	Nicotinamide adenine dinucleotide phosphate (NADP)	**1.05**	**0.01**	0.74	0.10	0.97	0.12
	Uridine 5′-diphospho-N-acetylgalactosamine	0.23	0.66	0.11	0.83	0.79	0.44
	S-Methyl-5′-thioadenosine	**1.64**	**1.93E-16**	0.51	0.27	**1.08**	**0.01**
Phenols	Matairesinol	0.30	0.50	0.44	0.35	**1.33**	**1.00E-03**
	5-Hydroxytryptophol (5HTOL)	0.07	0.88	0.23	0.63	0.35	0.47
	Phloretin	**1.28**	**4.55E-04**	**1.50**	**2.01E-05**	0.93	0.04
	Resveratrol	**1.58**	**4.00E-09**	**1.15**	**0.01**	**1.74**	**7.32E-10**

(*continued on next page*)

Table 1 (*continued*)

Metabolite		PS/TS		P × P/P × T		T × T/T × P	
		VIP	*P*.value	VIP	*P*.value	VIP	*P*.value
Other organic acids	Pantothenate	0.93	0.02	**1.41**	**1.32E-04**	**1.07**	**0.01**
	Pyroglutamic acid	0.45	0.30	**1.23**	**2.51E-03**	**1.51**	**3.46E-05**
	Caffeic Acid	**1.20**	**1.41E-03**	**1.31**	**2.53E-03**	**1.46**	**1.32E-04**
	Citrate	**1.35**	**1.17E-04**	0.85	0.06	0.21	0.67
	Mesaconic acid	0.41	0.35	0.26	0.58	**1.43**	**0.04**
	Methylmalonic acid	**1.59**	**4.77E-09**	**1.14**	**0.01**	**1.71**	**0.01**
	N-Methylanthranilic acid	0.16	0.72	**1.53**	**6.98E-06**	**1.76**	**3.20E-11**
	Salicylic acid	**1.57**	**1.12E-08**	**1.81**	**3.38E-13**	**1.67**	**0.01**
	Anthranilic acid (Vitamin L1)	**1.59**	**1.28E-09**	**1.63**	**8.63E-08**	**1.64**	**6.33E-07**
	3-Phenylpropanoic acid	0.11	0.82	**1.09**	**0.01**	0.03	0.94
	Dihydroxyfumarate	**1.12**	**4.03E-03**	**1.00**	**0.02**	0.92	0.04
	3-Hydroxy-3-methylglutaric acid	0.90	0.03	0.55	0.25	**1.64**	**0.01**
	2-Hydroxyphenylacetic acid	**1.56**	**6.52E-08**	0.14	0.73	1.29	0.17
	4-Hydroxybenzoate	0.69	0.10	0.11	0.85	0.10	0.75
	Galactonic acid	**1.11**	**4.11E-03**	0.29	0.59	0.43	0.94
	Isocitrate	0.26	0.62	0.04	0.89	1.42	0.05
	Maleic acid	**1.15**	**2.66E-03**	0.45	0.37	0.70	0.36
	Malic acid	**1.07**	**0.01**	0.19	0.72	0.11	0.61
	Aconitate	0.54	0.21	0.46	0.32	0.14	0.78
	N-Acetyl-L-alanine	**1.59**	**1.64E-09**	**1.08**	**0.02**	**2.02**	**0.01**
	Ethylmalonic acid	0.63	0.15	0.09	0.87	**1.90**	**8.78E-04**
	4-Methoxycinnamic acid	**1.63**	**9.85E-13**	**1.54**	**6.60E-06**	**1.78**	**1.87E-14**
	4-Hydroxycinnamic acid	**1.03**	**0.01**	0.62	0.18	0.02	0.96
	Chlorogenic acid	0.44	0.32	0.47	0.31	0.93	0.04
	Isoferulic acid	**1.43**	**1.20E-05**	**1.25**	**1.67E-03**	0.73	0.12
	trans-2-Hydroxycinnamic acid	0.02	0.96	0.92	0.04	1.17	0.08
	m-Coumaric acid	0.63	0.14	0.13	0.79	**1.20**	**4.78E-03**
	Citramalic acid	0.74	0.09	0.14	0.76	0.49	0.52
	3-Hydroxybenzoate	0.28	0.53	0.88	0.05	0.13	0.79
	Homocitrate	0.43	0.31	0.91	0.06	0.23	0.91
	Xanthurenic acid	**1.41**	**2.27E-05**	0.72	0.11	0.63	0.18
	meso-Tartaric acid	**1.60**	**1.79E-10**	0.01	0.97	0.58	0.26
	Tartaric acid	**1.01**	**0.01**	0.34	0.49	0.48	0.79
	Vanillic acid	**1.04**	**0.01**	**1.44**	**8.16E-05**	**1.65**	**9.84E-11**
Fatty acids (derivatives)/lipids	16-Hydroxypalmitic acid	**1.54**	**8.84E-08**	**1.14**	**0.01**	**1.60**	**0.01**
	Oleic acid	0.99	0.02	**1.69**	**2.16E-07**	1.06	0.16
	Linoleic acid	**1.32**	**2.58E-04**	**1.30**	**9.25E-04**	0.23	0.63
	Palmitic acid	0.73	0.08	**1.63**	**2.89E-06**	0.93	0.26
	Pimelic acid	0.52	0.22	**1.45**	**1.99E-04**	0.57	0.60
	Traumatic Acid	0.68	0.13	**1.72**	**9.86E-08**	0.73	0.23
	3-Hydroxycapric acid	**1.27**	**3.95E-04**	0.59	0.25	1.17	0.07
	5-Methoxypsoralen	**1.52**	**2.68E-07**	0.14	0.75	0.62	0.35
	all cis-(6,9,12)-Linolenic acid	**1.06**	**0.01**	**1.81**	**1.66E-13**	**1.79**	**0.02**
	alpha-Linolenic acid	0.40	0.34	0.29	0.56	0.48	0.25
	Azelaic acid	0.81	0.05	3.19E-03	0.99	0.30	0.54
	Suberic acid	**1.59**	**2.86E-09**	0.96	0.03	0.96	0.14
	Sebacic acid	**1.38**	**4.41E-05**	0.22	0.61	0.91	0.12
	5-Hydroxyhexanoic acid	0.85	0.04	0.48	0.31	0.11	0.82
	Jasmine lactone	0.31	0.48	0.46	0.33	**1.79**	**2.47E-16**
	Pristanic acid	0.77	0.07	**1.34**	**4.92E-04**	**1.58**	**4.95E-06**
	(4Z,7Z,10Z,13Z,16Z,19Z)-4,7,10,13,1 6,19-Docosahexaenoic acid	0.78	0.06	0.91	0.04	**1.26**	**2.45E-03**
	cis-9-Palmitoleic acid	0.12	0.78	**1.68**	**3.24E-09**	**1.19**	**0.01**
	LysoPC(16:0)	**1.46**	**4.27E-06**	**1.44**	**8.77E-05**	**1.54**	**2.05E-05**
	LysoPC(18:0)	**1.46**	**4.78E-06**	**1.32**	**6.97E-04**	**1.35**	**6.95E-04**
	LysoPC(18:1(9Z))	**1.44**	**1.08E-05**	**1.62**	**1.60E-07**	**1.26**	**2.27E-03**
	PA(16:0/18:1(9Z))	**1.42**	**7.61E-06**	**1.77**	**1.39E-09**	**2.25**	**1.83E-04**
	PA(16:0/18:2(9Z,12Z))	**1.24**	**5.62E-04**	**1.63**	**4.02E-06**	**2.04**	**9.66E-04**
	LPA(18:1(9Z)/0:0)	**1.48**	**1.64E-06**	**1.64**	**2.44E-06**	**1.32**	**1.19E-03**
	PC(16:0/16:0)	0.51	0.25	0.59	0.20	0.13	0.79
	MG(16:0)	0.21	0.65	0.09	0.83	0.63	0.18
	LysoPE(16:0/0:0)	**1.46**	**5.21E-06**	**1.29**	**1.04E-03**	**1.47**	**1.13E-04**
	Palmitoylethanolamide	0.24	0.59	**1.08**	**0.01**	0.32	0.51
	1-Oleoyl-sn-glycerol 3-phosphate	**1.14**	**3.00E-03**	**1.69**	**7.65E-10**	**1.68**	**7.15E-08**
	1-Stearoyl-sn-glycerol 3-phosphocholine	**1.60**	**5.98E-10**	0.02	0.95	0.98	0.03
	Erucamide	**1.46**	**5.39E-06**	**1.68**	**1.42E-09**	**1.59**	**5.14E-06**
Alcohols	Phytosphingosine	**1.41**	**2.20E-05**	**1.66**	**1.63E-08**	**1.65**	**5.21E-07**
	Uvaol	**1.05**	**0.01**	**1.63**	**9.77E-08**	**1.64**	**4.70E-07**
	Ascorbic acid	**1.60**	**5.50E-10**	0.78	0.10	0.09	0.62
	25-hydroxyvitamin D3	0.65	0.13	0.77	0.09	**1.58**	**5.77E-06**

(*continued on next page*)

Table 1 (*continued*)

Metabolite		PS/TS		P × P/P × T		T × T/T × P	
		VIP	*P*.value	VIP	*P*.value	VIP	*P*.value
Aldehydes	Phenylacetaldehyde	0.07	0.88	0.43	0.36	**1.14**	**0.01**
	Vanillin	**1.64**	**4.19E-15**	**1.70**	**1.58E-10**	**1.69**	**4.66E-17**
Amines	3-Methoxytyramine	0.42	0.33	0.09	0.84	**1.71**	**1.21E-08**
	Spermidine	**1.60**	**8.47E-10**	**1.36**	**3.21E-04**	**1.71**	**1.21E-08**
	Betaine	**1.61**	**6.76E-11**	**1.70**	**4.23E-11**	0.96	0.03
	Glycerophosphocholine	**1.62**	**3.11E-11**	**1.50**	**1.89E-05**	0.51	0.29
	Tryptamine	0.43	0.33	**1.69**	**3.18E-10**	**1.45**	**2.26E-05**
	Phenylethylamine	**1.26**	**5.76E-04**	0.64	0.16	0.79	0.09
	Tyramine	0.17	0.71	0.52	0.27	**1.02**	**0.02**
Alkaloids	Caffeine	**1.63**	**2.87E-13**	0.61	0.18	0.79	0.08
	3-Methyluric acid	**1.31**	**1.21E-04**	**1.16**	**0.01**	1.49	0.10
	Theobromine	**1.02**	**0.01**	**1.54**	**6.30E-06**	0.20	0.68
	Uric acid	0.94	0.02	0.69	0.16	**1.72**	**0.02**
Other compounds	Indole	**1.20**	**1.42E-03**	0.68	0.14	0.32	0.52
	3-Formylindole	**1.35**	**1.11E-04**	0.76	0.09	**1.26**	**2.23E-03**
	Biliverdin	0.76	0.07	0.61	0.18	**1.01**	**0.02**

*Variables with VIP (Variable Importance in the Projection) > 1 means they(variables) play significant roles in the classification. The *P* value ($P < 0.05$ means the metabolites with significant differences. Bold number means metabolites with significant changes (VIP > 1,$P < 0.05$).

many related pathways. After successful recognition, energy-related nutrients must be metabolized to produce acetyl-CoA, which is incorporated into the pollen tube's TCA cycle, ultimately enhancing ATP production to promote pollen tube growth (Yue et al., 2014). The superpathway is composed of many metabolites that construct a style metabolic network with annotated pathway information in KEGG. After germination, the pollen tube grows into the extracellular matrix in the stigma secretory zone, and pistil transmitting tract cells secrete amino acids, soluble sugar (sucrose) and phenols into the extracellular matrix, providing nutrients and resources that support rapid pollen germination and pollen tube growth after the materials stored within the pollen grain are exhausted (Goetz et al., 2017; Labarca and Loewus, 1973). Moreover, the TCA intermediates and amino acids/peptides remained higher in SI pollination than in SC pollination in both the T and P groups. Without pollen growth, metabolites remain at a relatively high level. Zhao asserted that tomato SI might be due to lack of energy nutrients for pollen growth (Zhao et al., 2016). However, the results of our research indicate that HetSI might not be related to a lack of energy nutrients to facilitate pollen tube growth, which is completely different from Zhao's hypothesis regarding the self-incompatibility mechanism of tomatoes.

Surprisingly, the total levels of flavonoids, other organic acids, fatty acids (derivatives)/lipids, phenols and amines changed in an opposite way in the P and T groups: the content was higher in SI samples than in SC samples in the T group, but the opposite was found in the P group. This result might be due to the extremely complex mechanism and growth rate variation of pollen tubes. Genetic and genomic approaches have shown that initial pollen tube growth is autotrophic and utilizes the nutrients stored in pollen grains; for subsequent growth, heterotrophic pollen tubes absorb and metabolize external energy-rich metabolites from the stigma for energy generation (ATP) (Labarca and Loewus, 1973; Obermeyer et al., 2013). After rehydration, metabolites in pollen are quickly reformed due to enzyme reactivation (Fila et al., 2016; Rotsch et al., 2017). According to our fluorescence microscopy results, pollen germination was delayed in P × T pollinations, and no pollen tube was observed, which may result in metabolic differences due to the variation in pollen tube growth capacity. Compared with the metabolites in the desiccated pollen in the SI group of the P group, the metabolites in rehydrated pollen in the SC group might have accumulated to support the initial autotrophic stage of pollen tube growth. On the other hand, growing pollen tubes may also consume energy-related nutrients from the style (Yue et al., 2014), including flavonoids, other organic acids, fatty acids (derivatives)/lipids, phenols and amines. Thus, the sharp decline in SC pollinations in the T group might be due to the consumption of supplements for pollen tube growth.

In addition, cell wall loosening in the stigma is important for pollen tube growth (Elleman et al., 1992) and flavonoids are essential for pollen germination and tube growth and may be involved in cell wall loosening, thus facilitating penetration of the SC stigma by the pollen tube and consequently the supply of flavonoids by either the pollen or stigma at pollination. For instance, kaempferol increased in SC samples when pollen tubes grew into the pistil-transmitting tissue. This result is consistent with previously reported results for *petunia* (Taylor and Jorgensen, 1992; Ylstra et al., 1994; Vogt et al., 1995). Lipids play an important role in the hydrophobic nature of pollen-stigma capture (Heizmann et al., 2000). PA (phosphatidic acid) is a kind of glycerophospholipid that is important for membrane signaling during pollen tube growth (Potocký et al., 2003). PA(16:0/18:1(9Z)) and PA(16:0/18:2(9Z,12Z)) were present at high levels in SC pollinations to facilitate pollen tube growth.

5. Conclusions

In this research, we investigated the morphological and metabolic differences in different types of styles and SC and SI pollinations of *Plumbago auriculata*. Metabolic discrimination between SC and SI during pollen tube growth by UPLC-MS/MS in HetSI plants has not been reported previously. A total of 142 chemical compounds were identified. The metabolites were primarily distributed 11 chemical classes, including amino acids/peptides, flavonoids, phenols, glycosides/sugars, other organic acids, fatty acids (derivatives)/lipids, amines, aldehydes, alkaloids, alcohols and other compounds. The metabolomes of PS, TS, P × P, P × T, T × T, and T × P pollinations exhibited distinct metabolic changes. There was an abundance of amino acids/peptides and tricarboxylic acid cycle-related metabolites in SI pollinations, suggesting that the lack of energy nutrients might not be the source of self-incompatibility. The growth rate differences of the pollen tube might also result in metabolic differences in PS and TS. These results provide supplementary data for HetSI as well as a basis for prospective works.

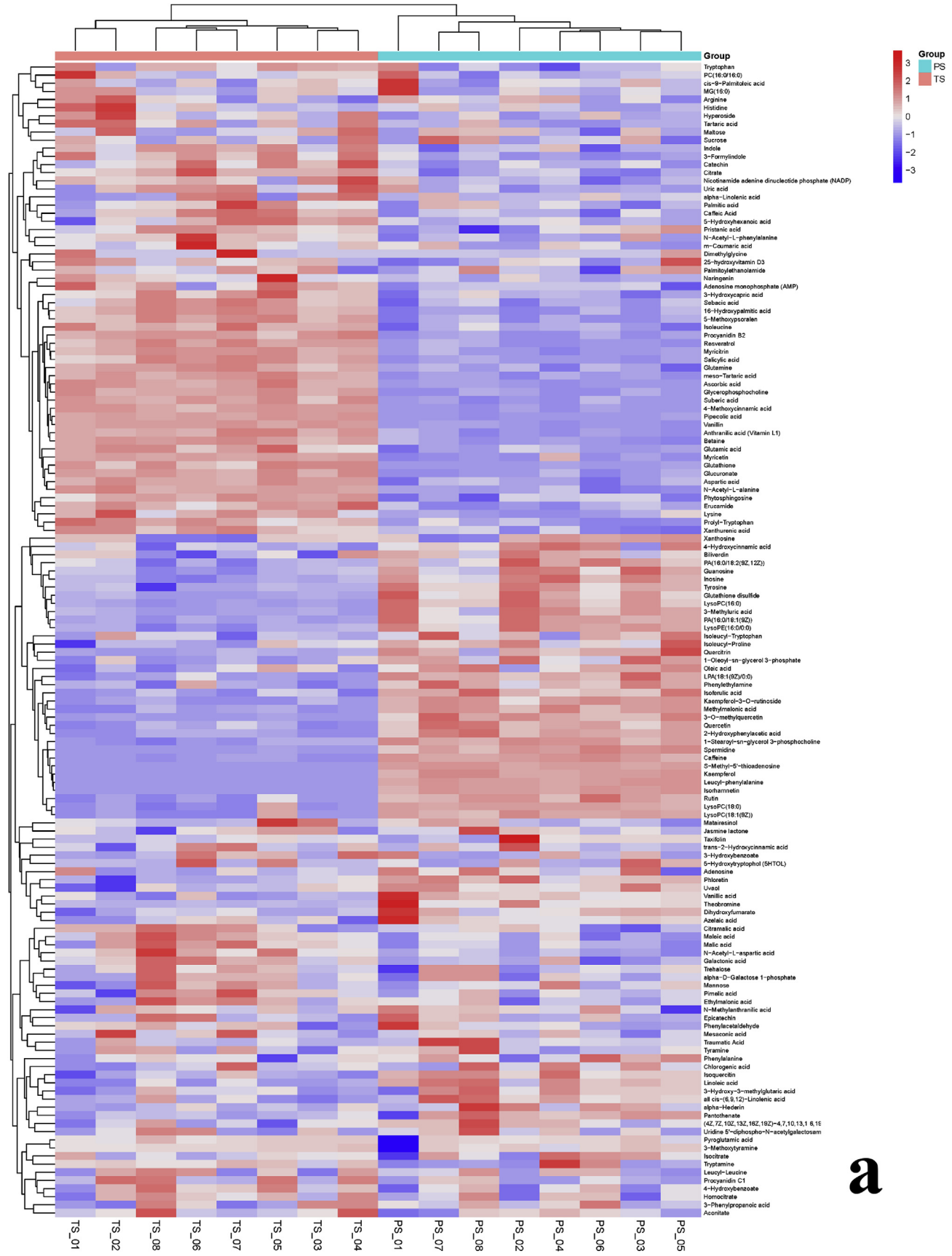

Fig. 6. Heatmaps of different pollinations in PS,TS (a) and P × P, P × T, T × T, T × P(b).

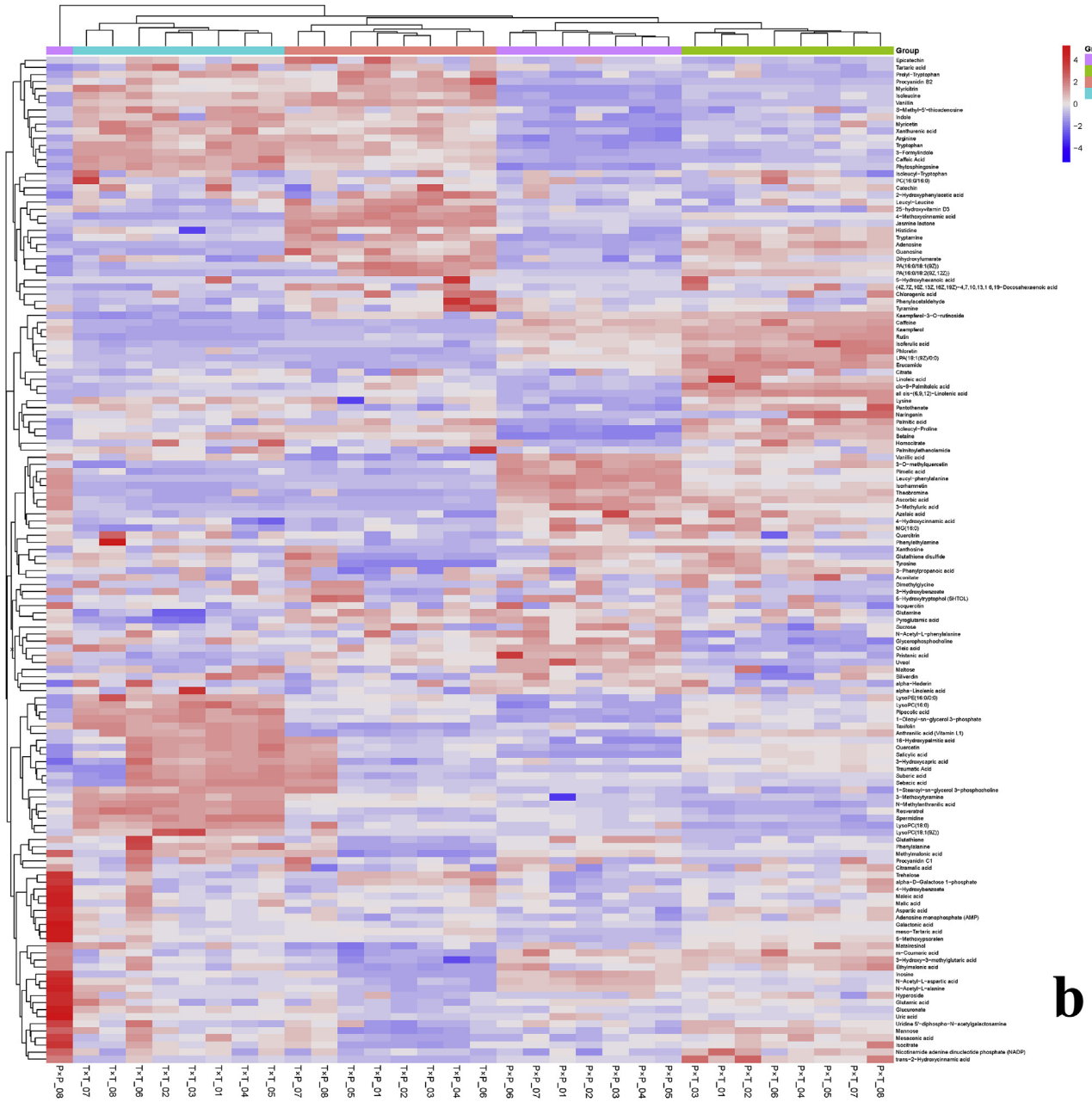

Fig. 6. (*continued*)

Author contributions

Experimental design, Suping Gao and Ting Lei. Experiment and result analysis, Di Hu and Wenji Li. Experimental verification, Ju Hu. Paper writing, Di Hu and Wenji Li. Tabulation, Ping Shen and Yurong Li. Revision, Jiani Li.

Funding

The study was supported by the National Key R&D Program of China (2018YFD0600105) and the Sichuan Science and Technology Program (2018JY0211).

Ethics approval and consent to participate

Not applicable.

Consent for publication

Not applicable.

Availability of data and material

All data generated or analyzed during this study are included in this published article [and its supplementary information files].

Declaration of Competing Interest

The authors declare that they have no known competing financial interests or personal relationships that could have appeared to influence the work reported in this paper.

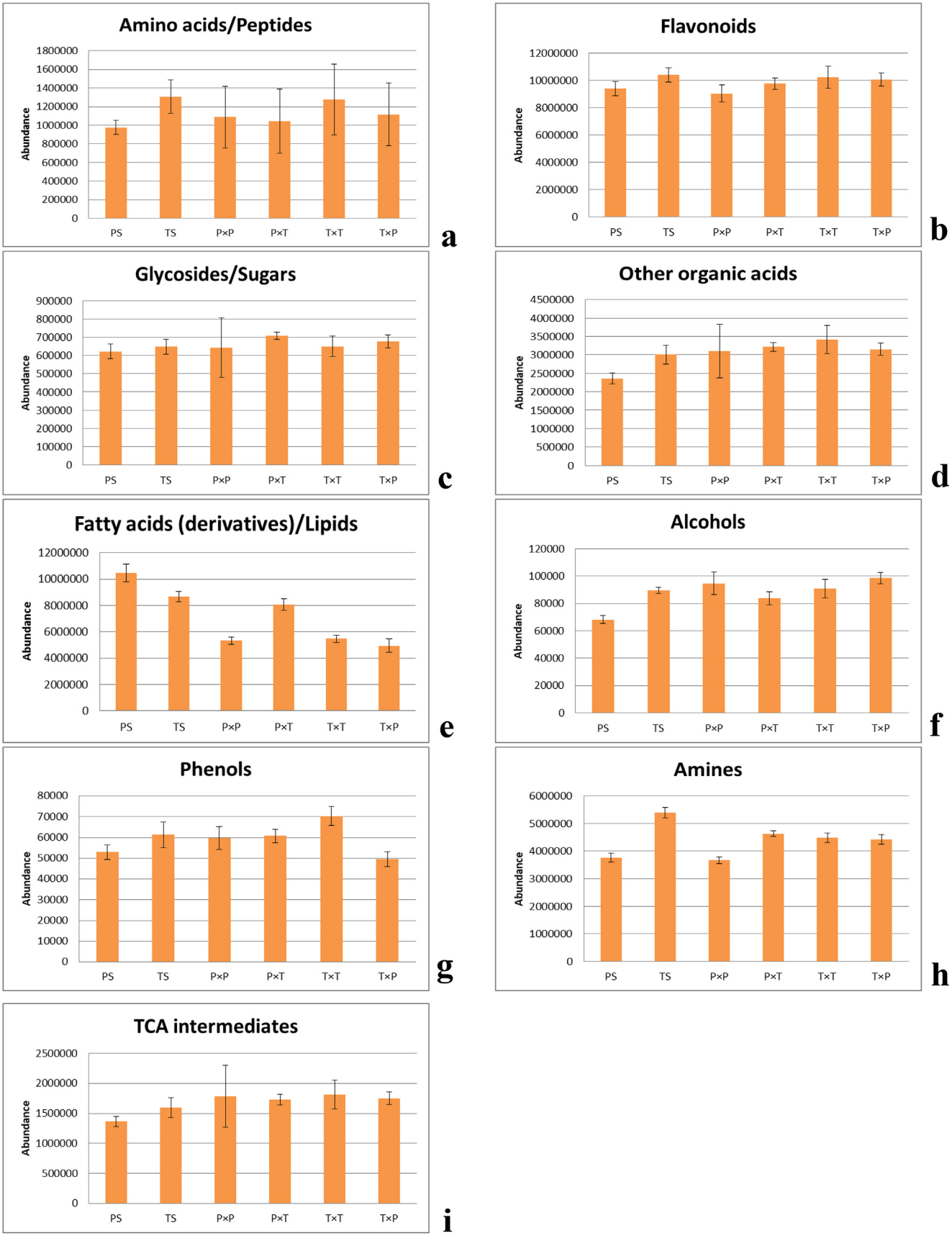

Fig. 7. Histograms showing differences in metabolite contents in different pollinations: (a) amino acids/peptides; (b) flavonoids; (c) glycosides/sugars; (d) other organic acids; (e) fatty acids (derivatives)/lipids; (f) alcohols; (g) phenols; (h) amines; (i) TCA intermediates.

Appendix A. Supplementary data

Supplementary data to this article can be found online at https://doi.org/10.1016/j.plaphy.2019.10.010.

References

Baker, H.G., 1953a. Dimorphism and monomorphism in the Plumbaginaceae. II. Pollen and stigmata in the genus *Limonium*. Ann. Bot. 17, 433–446.

Baker, H.G., 1953b. Dimorphism and monomorphism in the Plumbaginaceae. III. Correlation of geographical distribution patterns with dimorphism and monomorphism in *Limonium*. Ann. Bot. 17, 615–627.

Barrett, S.C., 1992. Evolution and Function of Heterostyly. Springer, Berlin, Heidelberg.

Barrett, S.C.H., Cruzan, M.B., 1994. Incompatibility in heterostylous plants. In: Williams, E.G., Clarke, A.E., Knox, R.B. (Eds.), Genetic Control of Self-Incompatibility and Reproductive Development in Flowering Plants. Advances in Cellular and Molecular Biology of Plants. Springer, Dordrecht, Netherlands, pp. 189–219.

Burrows, B.A., McCubbin, A.G., 2017. Sequencing the genomic regions flanking S-linked PvGLO sequences confirms the presence of two GLO loci, one of which lies adjacent to the style-length determinant gene CYP734A50. Plant Reprod. 30, 53–67.

Costa, J., Torices, R., Barrett, S.C.H., 2019. Evolutionary history of the buildup and breakdown of the heterostylous syndrome in Plumbaginaceae. New Phytol. https://doi.org/10.1111/nph.15768.

Darwin, C., 1862. On the Various Contrivances by Which British and Foreign Orchids Are Fertilised by Insects: and on the Good Effects of Intercrossing. John Murray, London, UK.

Dulberger, R., 1975. Intermorph structural differences between stigmatic papillae and pollen grains in relation to incompatibihty in Plumbaginaceae. P. Roy. Soc. Lond B Bio. 188, 257–274.

Elleman, C.J., Franklin-Tong, V., Dickinson, H.G., 1992. Pollination in species with dry stigmas: the nature of the early stigmatic response and the pathway taken by pollen tubes. New Phytol. 121, 413–424.

Faehnrich, B., Kraxner, C., Kummer, S., Franz, C., 2015. Pollen tube growth and self incompatibility in *Matricaria recutita*. Euphytica 206, 357–363.

Fernie, A.R., 2007. The future of metabolic phytochemistry: larger numbers of metabolites, higher resolution, greater understanding. Phytochemistry 68, 2861–2880.

Fiehn, O., 2002. Metabolomics - the link between genotypes and phenotypes. Plant Mol. Biol. 48, 155–171.

Fila, J., Radau, S., Matros, A., Hartmann, A., Scholz, U., Fecikova, J., Mock, H.P., Capkova, V., Zahedi, R.P., Honys, D., 2016. Phosphoproteomics profiling of tobacco mature pollen and pollen activated *in vitro*. Mol. Cell. Proteom. 15, 1338–1350.

Franchi, G.G., Nepi, M., Matthews, M.L., Pacini, E., 2007. Anther opening, pollen biology and stigma receptivity in the long blooming species, *Parietaria judaica* L. (Urticaceae). Flora Morphol. Distrib. Funct. Ecol. Plants 202, 118–127.

Goetz, M., Guivarch, A., Hirsche, J., Bauerfeind, M.A., Gonzalez, M.C., Hyun, T.K., Eom, S.H., Chriqui, D., Engelke, T., Grosskinsky, D.K., Roitsch, T., 2017. Metabolic control of tobacco pollination by sugars and invertases. Plant Physiol 173, 984–997.

Heizmann, P., Luu, D.T., Dumas, C., 2000. Pollen-stigma adhesion in the *Brassicaceae*. Anna. Bot. 85, 23–27.

Hernández-Ledesma, P., Berendsohn, W.G., Borsch, T., von Mering, S., Akhani, H., Arias, S., Castañeda-Noa, I., Eggli, U., Eriksson, R., Flores-Olvera, H., Fuentes-Bazán, S., Kadereit, G., Klak, C., Korotkova, N., Nyffeler, R., Ocampo, G., Ochoterena, H., Oxelman, B., Rabeler, R.K., Sanchez, A., Schlumpberger, B.O., Uotila, P., 2015. A taxonomic backbone for the global synthesis of species diversity in the angiosperm order *Caryophyllales*. Willdenowia 45, 281–383.

Jiao, Y., Bai, Z., Xu, J., Zhao, M., Khan, Y., Hu, Y., Shi, L., 2018. Metabolomics and its physiological regulation process reveal the salt-tolerant mechanism in *Glycine soja* seedling roots. Plant Physiol. Biochem. 126, 187–196.

Kim, H.K., Choi, Y.H., Verpoorte, R., 2011. NMR-based plant metabolomics: where do we stand, where do we go? Trends Biotechnol. 29, 267–275.

Kohn, J.R., Barrett, S.C.H., 1992. Experimental studies on the functional significance of heterostyly. Evolution 46, 43–55.

Labarca, C., Loewus, F., 1973. The nutritional role of pistil exudate in pollen tube wall formation in *Lilium longiflorum*: II. Production and utilization of exudate from stigma and stylar canal. Plant Physiol 52, 87–92.

Lloyd, D.G., Webb, C.J., 1992. The evolution of heterostyly. In: Barrett, S.C.H. (Ed.), Evolution and Function of Heterostyly. Springer, Berlin, Heidelberg, pp. 151–178.

Lu, W., Bian, X., Yang, W., Cheng, T., Wang, J., Zhang, Q., Pan, H., 2018. Transcriptomics investigation into the mechanisms of self-incompatibility between Pin and thrum morphs of *Primula maximowiczii*. Int. J. Mol. Sci. 19, 1840.

Luu, D.T., Marty-Mazars, D., Trick, M., Dumas, C., Heizmann, P., 1999. Pollen-stigma adhesion in *Brassica* spp involves SLG and SLR1 glycoproteins. Plant Cell 11, 251–262.

Mondragon, M., John-Arputharaj, A., Pallmann, M., Dresselhaus, T., 2017. Similarities between reproductive and immune pistil transcriptomes of *Arabidopsis* species. Plant Physiol 174, 1559–1575.

Mucina, L., Hammer, T., 2019. *Limonium dagmarae* (Plumbaginaceae), a new species from Namaqualand coast, South Africa. Phytotaxa 403, 071–085.

Obermeyer, G., Fragner, L., Lang, V., Weckwerth, W., 2013. Dynamic adaption of metabolic pathways during germination and growth of lily pollen tubes after inhibition of the electron transport chain. Plant Physiol 162, 1822–1833.

Pacini, E., Guarnieri, M., Nepi, M., 2006. Pollen carbohydrates and water content during development, presentation, and dispersal: a short review. Protoplasma 228, 73–77.

Potocký, M., Eliáš, M., Profotová, B., Novotná, Z., Valentová, O., Žárský, V., 2003. Phosphatidic acid produced by phospholipase D is required for tobacco pollen tube growth. Planta 217, 122–130.

Rotsch, A.H., Kopka, J., Feussner, I., Ischebeck, T., 2017. Central metabolite and sterol profiling divides tobacco male gametophyte development and pollen tube growth into eight metabolic phases. Plant J. 92, 129–146.

Samuel, M.A., Chaal, B.K., Lampard, G., Green, B.R., Ellis, B.E., 2008. Surviving the passage: non-canonical stromal targeting of an *Arabidopsis* mitogen-activated protein kinase kinase. Plant Signal. Behav. 3, 6–12.

Stevens, V.A., Murray, B.G., 1981. Studies on heteromorphic self-incompatibility systems: the cytochemistry and ultrastructure of the tapetum of *Primula obconica*. J. Cell Sci. 50, 419–431.

Swanson, R., Edlund, A.F., Preuss, D., 2004. Species specificity in pollen-pistil interactions. Annu. Rev. Genet. 38, 793–818.

Takeshima, R., Nishio, T., Komatsu, S., Kurauchi, N., Matsui, K., 2019. Identification of a gene encoding polygalacturonase expressed specifically in short styles in distylous common buckwheat (*Fagopyrum esculentum*). Heredity. https://doi.org/10.1038/s41437-019-0227-x.

Taylor, L.P., Jorgensen, R., 1992. Conditional male fertility in chalcone synthase-deficient *Petunia*. J. Hered. 83, 11–17.

Vogt, T., Wollenweber, E., Taylor, L.P., 1995. The structural requirements of flavonols that induce pollen germination of conditionally male fertile *Petunia*. Phytochemistry 38, 589–592.

Ylstra, B., Busscher, J., Franken, J., Hollman, P.C.H., Mol, J.N.M., van Tunen, A.J., 1994. Flavonols and fertilization in *Petunia hybrida*: localization and mode of action during pollen tube growth. Plant J. 6, 201–212.

Yue, X., Gao, X.Q., Wang, F., Dong, Y., Li, X., Zhang, X.S., 2014. Transcriptional evidence for inferred pattern of pollen tube-stigma metabolic coupling during pollination. PLoS One 9, e107046.

Zhang, Y., Ma, X.M., Wang, X.C., Liu, J.H., Huang, B.Y., Guo, X.Y., Xiong, S.P., La, G.X., 2017. UPLC-QTOF analysis reveals metabolomic changes in the flag leaf of wheat (*Triticum aestivum* L.) under low-nitrogen stress. Plant Physiol. Biochem. 111, 30–38.

Zhao, P., Pan, Q., Yu, W., Zhao, L., 2016. Dissect style response to pollination using metabolite profiling in self-compatible and self-incompatible tomato species. J. Chromatogr. B Analyt. Technol. Biomed. Life Sci. 1017–1018, 153–162.